Nanoscale

Rapid and Sensitive Detection of Cardiac Troponin I using a Force Enhanced Immunoassay with Nanoporous Membrane

Journal:	*Nanoscale*
Manuscript ID	NR-ART-03-2020-002234.R1
Article Type:	Paper
Date Submitted by the Author:	23-May-2020

Complete List of Authors:	Chang, Won-suk; Purdue University, Schools of Chemical and Biomedical Engineering, Li, Peng; University College Dublin, School of Chemistry and Chemical Biology Kakade, Sandeep; Purdue University, Schools of Chemical and Biomedical Engineering Xiong, Ying; Purdue University, Schools of Chemical and Biomedical Engineering Shang, Hao; Purdue University, Schools of Chemical and Biomedical Engineering, Zhang, Yong; National Center for Nanoscience and Technology, Lee, Gil; University College Dublin, Chemistry; University College Dublin, Conway Institute of Biomolecular and Biomedical Research

ARTICLE

Rapid and Sensitive Detection of Cardiac Troponin I using a Force Enhanced Immunoassay with Nanoporous Membrane

Received 00th January 20xx,
Accepted 00th January 20xx

DOI: 10.1039/x0xx00000x

Won-Suk Chang[a,b] , Peng Li[c], Sandeep Kakade[a], Ying Xiong[a], Hao Shang[a], Yong Zhang[c] and Gil U Lee[a,c*]

There is a need for point of care diagnostic technologies that are rapid, sensitive, easy to use, and relatively inexpensive. In this article we describe an assay that uses an antibody functionalized nanoporous membrane and superparamagnetic beads to capture and detect human cardiac troponin I (cTnI), which is an important biomarker for acute myocardial infarction (AMI). The membrane assisted force differentiation assay (mFDA) is capable of detecting cTnI at a sensitivity of 0.1 pg/ml in 15% serum in less than 16 minutes, which is a significant improvement in performance over conventional lateral flow immuosorbant assays. The speed of this assay results from the rapid concentration of cTnI on the surface of the nanoporous membrane and the use of the magnetic beads to react with with the analyte, which rapidly react with the immobilized cTnI. The increased sensitivity of assay results from the the use of magnetically controlled forces that reduce the nonspecific background and modify both the on-rate and off-rate. We believe that the improved performance and ease of application of the mFDA will make it useful in the early identification of AMI as well as other diseases based on the detection of 1 pg/ml variations in the concentrations cTnI in blood.

Introduction

Highly specific biomarkers are becoming available for the diagnosis of diseases as a result of improved proteomic and genomic screening technologies and have the potential to significantly improve the quality of healthcare. An important example is troponin, a 23,876 Da protein, that plays an important role in the regulation of skeletal and cardiac muscle contraction[1]. Elevated levels of cTnI can be detected in a patient's blood 3-6 hours after the onset of chest pain, reaching a peak level within 16–30 hours. The European Society and American College of Cardiology now defines AMI based on measuring the levels of cTnI in the blood of patients presenting with symptoms of acute coronary syndrome[2]. There is a need for rapid, specific, and sensitive diagnostic devices for the identification of biomarkers, such as cTnI, in a point of care (POC) setting. Lateral flow immunoassays (LFIA) are the most commonly used form of diagnostic technology employed in a POC setting and is typically applied to detect analytes at the µg/ml level in 10-15 minutes[3]. Second generation POC technologies are now able to detect cTnI with sensitivities of < 40 ng/ml resulting in the diagnostics sensitivities of > 60%[4-8]. The background level of cTnI in healthy individuals is 10 pg/ml thus higher sensitivity cTnI POC tests would be very useful for more sensitive detection of AMI.

Troponin has also been identified as an important tool for risk stratification, as elevated cTnI levels correlates with the clinical severity of several important diseases and life expectancy[9]. CTnI's used as a clinical biomarker has been extended to include pathologies characterized by cardiac injury, including, unstable angina, left ventricular hypertrophy, congestive heart failure, pulmonary embolism, blunt trauma, sepsis, moderate renal disease, renal failure, diabetes mellitus, and cardiotoxicity associated with anticancer drugs and sympathomimetics. These diseases are not always associated with high levels of cTnI but with variations in the endogenous level. Thus, there appears to be a need for higher sensitivity cTnI POC tests to make it possible to rapidly identify cardiac injury associated with a number of diseases.

The development of single molecule biophysical techniques has made it possible to directly measure forces between and within individual macromolecules, and a number of these techniques have been applied to develop novel bioanalytical diagnostics[10-13]. The magnetic tweezers technique lends itself to biosensing because superparamagnetic (SPM) beads are commonly used for the separation of complex media and piconewton forces can be simultaneously transduced to many hundreds of thousands of beads[14-19]. In a force differentiation assay (FDA) the analyte is captured on a substrate based on the reaction with an immobilized receptor and detected through the binding of an antibody functionalized bead to the surface[20, 21]. The state of the SPM beads can be detected using optical[4, 21-23], chemical[24], or magnetic signals[11, 13, 25-27]. These techniques provide significant advance in the capability of bioanalytical systems, yet wider application of SPM beads is currently limited by three factors. First, some assays take an extended period of time to execute due to the multiple reaction and washing steps that require proteins to diffuse and react at a surface. Other assays have sensitivities limited to one to two orders of magnitude higher than conventional techniques, such as, ELISA, imposed by antigen-antibody equilibration. Third, some of the amplification and sensing techniques can be relatively expensive to implement due to the cost of reagents or manufacture of highly sensitive solid-state MEMs devices.

[a] *Schools of Chemical and Biomedical Engineering, Forney Hall, Purdue University, West Lafayette, IN 47907, USA.*
[b] *Material Research Center, Samsung Advanced Institute of Technology (SAIT), Suwon, 16678, South Korea.*
[d][c] *School of Chemistry and Conway Institute for Biomolecular and Biomedical Research, University College Dublin, Belfield, Dublin 4, Ireland.*
[c] *Corresponding author: gil.lee@ucd.ie*
Electronic Supplementary Information (ESI) available: [details of any supplementary information available should be included here]. See DOI: 10.1039/x0xx00000x

Figure 1A presents a schematic of the membrane assisted force differentiation assay (mFDA) that we have demonstrated for cTnI. In this assay the SPM beads (labelled **1**) bind to the analyte immobilized on the active surface of the membrane (labelled **4**) in a sandwich configuration. These membranes are produced by anodically etching aluminium and have a thin, dense layer of nanometer size pores on their active surface supported by a microporous layer[28, 29]. These membranes are easily integrated into lab on a chip devices due to their mechanical strength and chemical inertness[30]. Figure 1B presents a scheme of the surface chemistry that was used to specifically capture cTnI. The membrane and beads were functionalized with a dense monolayer of polyethylene glycol to minimize nonspecific protein adhesion due to the high concentration of blood proteins present in plasma (labelled **9**)[28]. The cTnI (**5**) was identified with monoclonal antibodies (labelled **6**, **7**, and **8**) that were covalently grafted to the poly (ethylene glycol) polymer (PEG) monolayers.

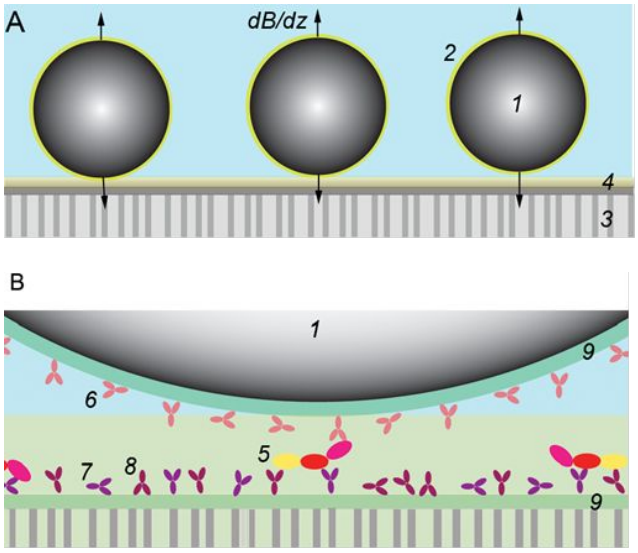

Figure 1. Schematic of membrane assisted force differentiation assay. **A.** Cross-sectional schematic of the mFDA with 1 µm diameter superparamagnetic bead (**1**) coated with antibody-PEG monolayer (**2**) reacted with an antibody (**4**) coated nanoporous alumina membrane (**3**). A controlled force can be applied to the beads with an external magnetic field (***B***) and gradient (***dB/dz***). **B.** Schematic of the point of contact of the bead with the membrane where the the cTnI (**5**) is concentrated on the membrane and detected with a magnetic bead (**1**). Monoclonal antibodies against cTnI (**6**,**7**, and **8**) are covalently grafted to the beads and membranes using a monolayer of PEG (**9**).

Results

Membrane Pore Structure

Figure 2 presents SEM micrographs of the active side of commercial 20 and 100 nm nominal pore size membranes that have been cleaned with HCl and NH_4OH:H_2O_2. Vigorous cleaning (etching) was found to be necessary to remove the significant amount of carbon-based contamination present on commercial membranes to enable reproducible functionalised membranes. Figure 2A shows that the pores on the active surface of the 20 nm membranes have an average size of 27 nm and were largely polygonal in shape with 3 to 6 sides. There were also structures on the active surface of the membrane that appear to result from the fusion of the network of smaller pores that occurs when the membranes are cleaned. The shape of the supporting membrane under the active surface can also be seen in these micrographs and it has pores of between 100 and 200 nm diameter. Cross-sectional images of the membranes confirmed that the smaller pores of the active surface span only approximately 100 nm of the membrane while large 100-200 nm diameter pores transverse most of the 60 µm of the membrane. This is consistent with the asymmetric design of these membranes aimed to maximize permeability[28, 31]. Figure 2B shows the pores of the active surface of the 100 nm membrane, which have a complex shape and average diameter of 156 nm. The shape of the active pores appears to be dominated by thin walls that span the supporting membrane.

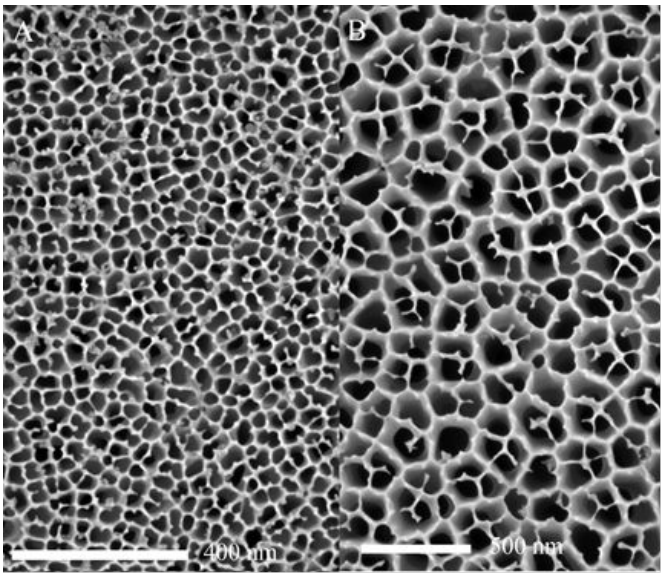

Fig. 2. Field emission SEM micrographs of the nanoporous alumina membranes after cleaning and coating with 20 nm of Pt. **A.** Top view of a typical 20 nm membrane after cleaning. **B.** Top view of 100 nm membrane after cleaning.

Table 1 summarizes the mean pore diameter, weighted average pore diameter, pore density, and pore area fraction of the active surface of the membranes measured from the SEM images. The weighted pore diameter and pore density were calculated to determine theoretical permeabilities of the membranes, and the local hydrodynamic conditions in the pores.

Table 1. Summary of the structure of 20 nm and 100 nm Anodisc® membrane. The pore diameter (***D***) is determined from the area (***A***) of the pore $D = \sqrt{\frac{4A}{\pi}}$ and the weighted average pore diameter is

determined from the distribution of pore sizes $\langle D_w \rangle = \sqrt[4]{\frac{\sum_{n=1}^{N} D_n^4}{N}}$,

where D_n is the pore diameter and N is the total number of pores. Likewise, pore density and pore area fraction are calculated by counting the number of pores and porous area over a series of images.

Nominal Pore Size (nm)	Mean Pore diameter (nm)	Weighted Average Pore Diameter (nm)	Pore Density (pores m^2)	Pore Area fraction
20	35 ± 7.8	37	5.4×10^{14}	0.37
100	147 ± 27	156	3.3×10^{13}	0.41

Surface Properties of the PEG Films

X-ray photoelectron spectroscopy (XPS) surveys and high-resolution spectra were collected on the active sapphire surfaces before and after each of the reaction steps. XPS analysis of the untreated sapphire surface indicated a clean surface while the nanoporous membranes had significant amounts carbon contamination and trace amounts of phosphorous and fluorine (data not shown). Analysis indicated that the surface contamination was largely removed from the commercial membranes by treatment with the HCl and NH_4OH:H_2O_2 solution.

Table 2 summarizes the chemical composition of a sapphire surface after functionalization with M-PEG, Boc-PEG, and a 1:4 mixed Boc:M-PEG-silane measured from high resolution XPS scans. The binding energies and relative amounts of the Al 2p, Si 2p, C 1s, N 1s, and O 1s peaks have been presented for bare sapphire and each of the chemistries. The peak measured at 285 eV was assigned to C 1s, while the carbon peak at 286.5 eV was attributed to PEG. The O 1s peaks measured at 528.5 eV and 530 eV were associated with the Al_2O_3 and PEG, respectively. The Si 2p peak at 103.3 eV was associated with the silane. The N 1s peak at 399.1 eV was associated with BOC-PEG and surface contamination. Three observations can be made regarding the composition of the PEG films in Table 2. First, the aluminium and oxygen stoichiometry of the sapphire surfaces was consistent with an Al_2O_3 surface chemistry. Second, the aluminium signal decreases after the membrane was reacted with silane-PEG, but never drops below 30%. This behaviour was consistent with formation of a monolayer film of silane-PEG formed on membrane surfaces[21]. Third, the amount of silicon, C-O carbon, and oxygen, associated with the PEG surface chemistries were also consistent with a thin monolayer film. The fact that the aluminium signal in the M-PEG monolayer was lower than the BOC-PEG monolayer suggests it formed a denser film. This was confirmed by ellipsometry. It also appears that both the M-PEG and BOC-PEG films are denser than the mixed BOC:M-PEG monolayer.

Coating thickness and refractive index were measured using a variable spectroscopic ellipsometer, and the Cauchy model was used to determine the thickness and optical constants of the PEG film on sapphire surfaces. Measurements were carried out at multiple angles of incidence (65-75^o by 5^o increments). The M-PEG, Boc-PEG, and the mixed M-PEG and Boc-PEG (4:1) film thickness were 1.66 nm (n=1.366), 0.88 nm (n=1.340), and 1.11 nm (n=1.375), respectively.

Table 2. Relative atomic composition and binding energy of specific elements determined by XPS on the unmodified, M-PEG modified, Boc-PEG modified, and mixed PEG modified sapphire surfaces

	Unmodified Surfaces	M-PEG Modified Surface	BOC-PEG Modified Surface	Mixed BOC-PEG: M-PEG
Al *2p*	35.6 %	30.0 %	34.2 %	34.8 %
sapphire				
Si *2p*	0.1%	1%	0.8%	1.4 %
C*1s*: CC, CH	11.3 %	8.15 %	9.1 %	7.7 %
C *1s*: C-O	0.0 %	11.2 %	6.9%	5.6 %
N *1s*	0.3%	1.6 %	1.8 %	1.6 %
O *1s* -*sapphire*	52.5 %	31.7 %	29.1 %	27.9 %
O *1s* C-O	0%	16.4%	18.1 %	10.2 %

Permeability of the Membranes

The permeability of the liquid solutions through the unmodified and methoxy-PEG-modified membranes was measured to determine if the PEG monolayers influenced the transport behaviour. Figure 3 presents the results of permeability measurements through the silane-PEG-modified membranes. The flow of PBST through the 20 and 100 nm membranes was found to be a linear function of pressure and the measured permeability of the membranes was 1.5×10^{-8} and 3.8×10^{-9} mPa^{-1}s^{-1}, respectively. These permeabilities were characteristic of transport dominated by the laminar flow of the PBST through the smallest diameter pores[31].

The transport of the 1% (v/v) fetal calf serum (FCS) solution through the 20 and 100 nm PEG-membrane was found to be a nonlinear function of pressure, i.e., it was observed to steadily decrease in value as the pressure of filtration increased. This behaviour is consistent with measurements of protein filtration through nanoporous membranes, and the decreased rate of flux of protein solution through the membrane, with pressure, has been attributed to the formation of a thin film of proteins on the surface of the membrane[32]. According to this model increased filtration pressure produces a thicker (or denser)

protein film resulting in a higher hydrodynamic resistance and lower permeability.

At higher concentrations of FCS the permeability of the membrane was not only a function of pressure but was highly dependent on the total amount of solution that was filtered. Figure 4 presents the flow-time behaviour of PBST and several concentrations of FCS through a 100 nm PEG modified membrane at 10 PSIG (or 68.95 kPa). The flow rate through this membrane can be seen to decrease with time and as the concentration of FCS increased. Interestingly there was a significant decrease in flow rate after just 10 seconds of filtration for 10% serum. At serum concentrations above 20% it appears that the flow of solution effectively ceases after approximately 10 seconds. Permeability measurements of FCS on unmodified alumina membranes produce similar nonlinear behaviour but the permeability was observed to decrease much more rapidly (see Supplementary Section).

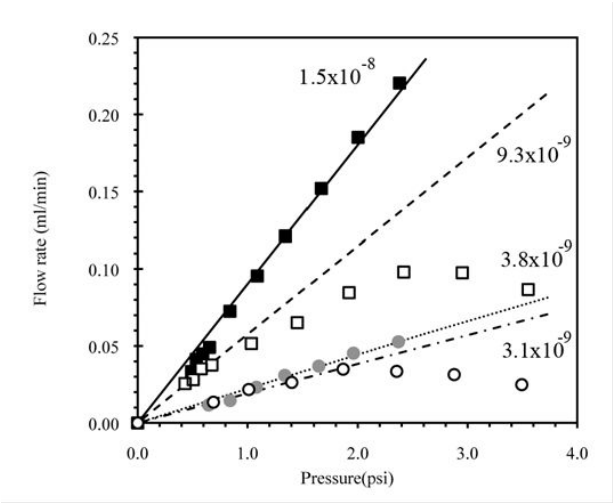

Fig. 3. Flow rate of PBST and 1% FCS in PBST through nanoporous alumina membranes that were modified with a PEG monolayer as a function of pressure. Four measurements are presented: ■ 100 nm membrane with PBST, □ 100 nm membrane with 1% FCS, ● 20 nm membrane with PBST, and ○ 20 nm membrane with 1% FCS. Lines present data used to calculate permeabilities, which are presented in mPa-1s-1. All measurement were carried out over a 5 minute period.

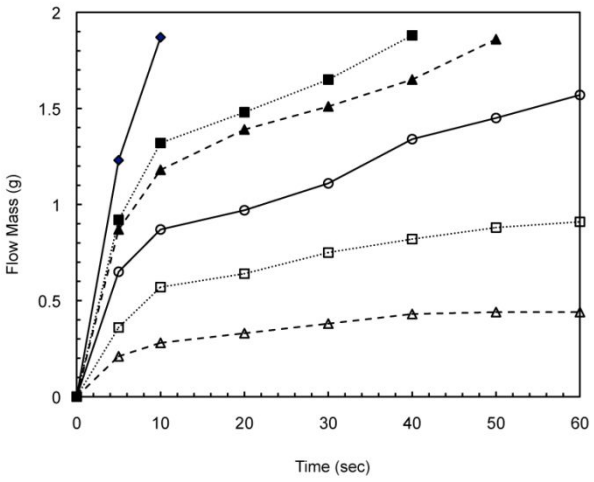

Fig. 4. Flow of FCS-PBST solutions across 100 nm PEG modified membranes 10 mm2 in size at 10 PSIG. Seven measurements are presented: ◆ Pure PBST, ■ 10% FCS in PBST, ▲ 15% FCS in PBST, ○ 20% FCS in PBST, □ 50% FCS in PBST, and △ 100% FCS.

A

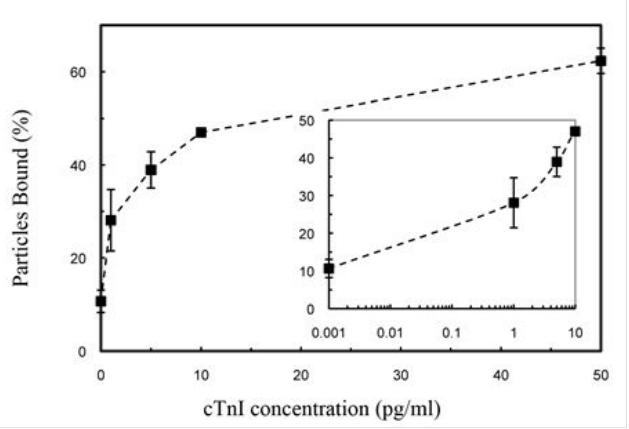

B

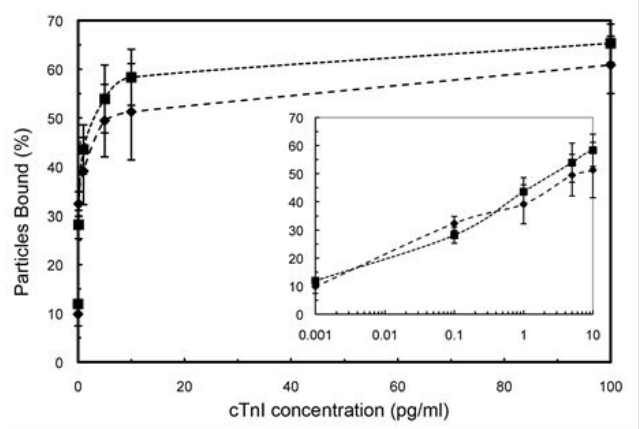

Fig. 5. Force differentiation response curves for cTnI assay for solid and nanoporous membrane substates. A. Sapphire surface (background 9±1). B. Nanoporous membranes ■ 100 nm (background 12±0.8) and ◆ 20 nm (background 10±2.4). Inset figures provide detailed information about the response of the assay

at fg/ml cTnI concentrations. These results were acquired using at least 3 sets of devices and include at least 6 devices.

cTnI Force Differentiation Assays in PBST

Force differentiation assays were conducted on PEG silane monolayers assembled on sapphire surfaces and nanoporous membranes to compare the sensitivity and response time of the membrane enhanced assay with an ELISA. Figure 5A presents the results of the FDA assays conducted on a sapphire surface and have the typically sigmoidal response curve expected from ELISA. This assay was conducted over a 90 minute period in which the sample was incubated with surface for 70 min, the surface was rinsed, the magnetic beads were added to the surface for 5 min, and the magnetic force was added for 1 min. For the purposes of this article we define sensitivity of an assay as the concentration at which the binding is two times the background of the assay. The background was measured to be 9±1% bound beads. The sensitivity of the assay was <1 pg/ml which is more than 3 orders of magnitude higher than that reported of conventional ELISAs using identical antibodies.

Figure 5B presents the results of mFDA cTnI assay on the nanoporous membranes in PBST. The sensitivity of the mFDA was found to be 0.1 pg/ml, which was similar to that on the sapphire surfaces. It also appears that the sensitivity of the mFDA was indistinguishable for the 20 and 100 nm membranes, indicating that the assay sensitivity was not highly dependent on the pore size of the membrane under these conditions. The mFDA were conducted over a 16 minute period in which the sample was added to the membrane for 10 minutes, the magnetic beads were added to the surface for 5 minutes, and the magnetic force was added for 1 minute.

cTnI Force Differentiation Assays in FCS

Figure 6A presents the result of a study of the sensitivity of the mFDA cTnI assay in 10% FCS as a function of the PEG surface chemistries. The ratio of BOC-PEG:M-PEG silane was varied from 1:1 to 1:9 in order to determine how the density of antibodies on the membrane influenced the nonspecific interaction of the beads with the membrane and the sensitivity of the FDA assay. High concentrations of BOC-PEG produced the highest senisitivity but also produced a background in excess of 30%. A background as low as 10% was achieved with surface chemistry of 1:9 BOC-PEG but there also was a decrease of the number of beads bound to the membranes after force differentiation at lower concentrations of cTnI. A 1:4 BOC:M-PEG was found to provided a reasonable level of bead binding while maintaining a the background below 11%.

Figure 6B presents the result of the cTnI assay run on the 1:4 BOC:M-PEG functionalized 100 nm membranes at four concentrations of FCS, i.e, 1, 10, 15, and 20%. The sensitivity sensitivities of the assays

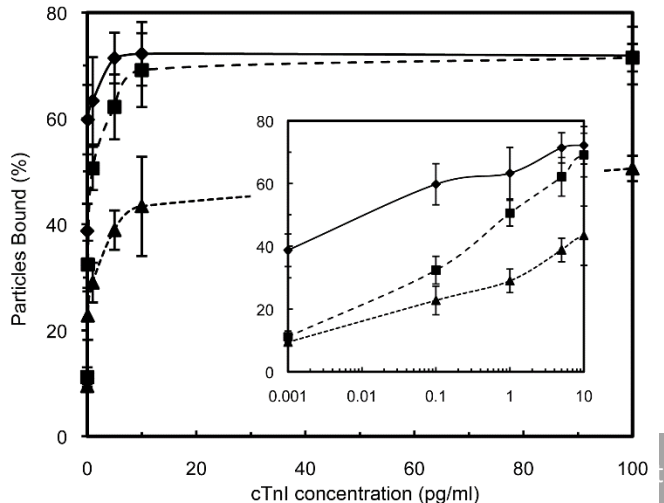

were similar except for the assays run in 20% FCS, which showed a significantly lower level of bead binding. The background of the assay also inceased at FCS concentrations greated greater than 15%. These resutls suggest that the mFDA assay works best in solutions of <15% FCS in PBST. The senstivity of the mFDA assay was 0.1 pg/ml in 15% FCS, which would be equivalent to a sensitiivity to 0.6 pg/ml of whole serum.

A

B

Fig. 6. Membrane enhanced force differentation assays for cTnI on 100 nm nanoporous membranes. A. Modification of surface chemistry ▲ 1:9 BOC:M-PEG (background 10□0.4), ■ 1:4 BOC:M-PEG (background 11±1.8), and ◆ 1:1 BOC:M-PEG (background 39±5). B. Nanoporous membrane functionalized 1:4 BOC:M-PEG: ■ 20% FCS (background 17±3.5), ◆ 15% FCS (background 10±2.6), ◇ 10% FCS (background 10±0.6) and ○ 1% FCS (background 11±1.8). Inset figures provide detailed information abou the response of the assay at fg/ml cTnI concentrations.

DISCUSSION

Membrane filtration

Our motivation for using a membrane in the mFDA was to increase the rate of reaction of cTnI with the substrate. Initial reflection on the filtration processes suggested that the amount

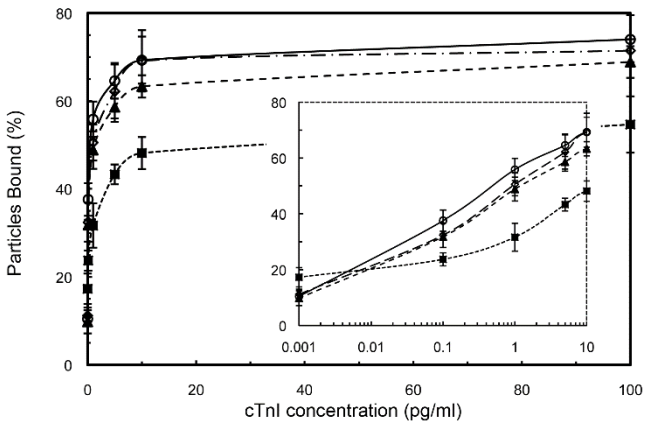

of analyte bound to a membrane, and thus the sensitivity of the assay, should be limited by the volume of sample filtered and the selectivity of the membrane. It was found that the sensitivity and specificity of the membrane assay was also highly dependent on the composition of the filtrate, surface chemistry of membrane, and pressure of filtration. In this section we consider the transport behaviour of the membrane to provide a rationale for the speed and sensitivity of the mFDA.

Figure 3 presents the flow rate of a protein free solution through the membranes as a function of pressure. The flow rate of the PBST measured through the membranes was a linear function of pressure, and the permeability of the 20 and 100 nm pore membranes was found to be 3.8×10^{-9} and 1.5×10^{-8} m/Pa•s, respectively. These permeabilities were consistent with the values previously measured on alumina membranes that had been modified with PEG-silane monolayers[21]. The flow rate of

a solvent through a parallel array of uniform, cylindrical pores under laminar conditions can be derived from Hagan-Poiseuille's' law

$$\frac{r^2}{8\mu\delta_m\phi},$$

where r is the pore radius, μ is viscosity, δ_m is the effective membrane thickness, and ϕ is the pore fraction, if one assumes pores pass directly through the membrane with the mean pore diameters. A theoretical permeability of 20 and 100 nm membranes can be calculated to be $1.5x10^{-9}$ and $2.0\ x10^{-9}$ m/Pa•s, respectively, if one uses the pore area fractions presented in Table 1. The theoretical permeabilities were somewhat smaller than the measured values, which we attribute to the asymmetric structure of the membrane. These results were quite encouraging in light of the fact that non-conformal polymer coatings have led to significantly decreased permeabilities[31].

Measurements of the flow rate of protein solution as a function of pressure illustrated that the transport was a nonlinear function of pressure, dependent on the fraction of FCS in solution, pressure, and time of filtration, as shown in Figure 3. Previous studies of ultrafiltration properties of dilute protein solutions have demonstrated that model proteins will rapidly pass through membranes if the ratio of protein-pore radius is less than 0.1.[33-35] Larger protein-to-pore size ratios will result in a rapid decrease in transport rates and proteins will be effectively retained on the membrane at ratios greater than 0.5. cTnI has a molecular weight of approximately 24 kDa and thus should readily pass through both the 20 and 100 nm pore membranes. Plasma is a complex media composed of approximately 92% water, 6-8% protein, 0.8 % salt, 0.6% lipids, and 0.1% (v/v) glucose. Each of these components will readily pass through the 100 nm membranes. Most of the protein components of serum will also readily pass through the 20 nm membranes with the exception of immunoglobins, which have an extended structure and molecular weights that range between 150-190 kDa. Theoretical considerations suggest that cTnI and plasma will pass through the 20 and 100 nm nanoporous membranes. It should be noted that protein aggregation of proteins, such as, albumin, in the serum must be minimized as it will lead to a significant decrease in filtration rates.

The FCS permeability measurements presented in Figure 4 clearly indicated that a factor other than simple pressure driven sieving determined the permeability rates. The accumulation of a protein rich layer at the membrane surface has previously been observed to influence the transport behaviour the membranes[32]. The properties of the protein layer is highly dependent on the filtration conditions, but it is clear that it will decrease permeability through at least three mechanisms, i.e., at low pressures the protein film will produce an osmotic pressure that counteracts pressure driven flow, and as the pressure increases the proteins will form a film on the membrane that would produce a hydrodynamic barrier to resist flow and ultimately irreversibly adsorb on the membrane resulting in membrane fouling. The measurement of the transport of 1% FCS through the membranes revealed two trends. First, at low pressures, i.e., approximately 2 PSIG, the rate of transport through both membranes was significantly lower than a PBST solution although it was still a linear function of pressure. At higher pressures the rate of flow became increasingly decoupled from the filtration pressure and was observed to decrease at pressure greater than 3 PSIG. This behaviour appears to be consistent with a change in transport behaviour due to the formation of a protein film on the membrane.

Figure 4 presents the filtration profile of a series of FCS solutions through the 100 nm membranes as a function of time at a pressure of 10 PSIG. A rapid decrease of total volume filtered is clearly observed between 15 and 50% FCS under this pressure. It was found empirically that 15% FCS produced a reasonable level of filtration, high specific bead binding, and low nonspecific bead binding. This suggests a dense, irreversibly adsorbed protein film does not form under these conditions. This sampling condition appears to be acceptable for both the 20 and 100 nm membranes, but it was found to be sensitive to the membrane surface chemistry, as described below.

We found that it was essential to avoid the formation of dense protein films on the nanoporous membranes in mFDA as they inhibit the binding of the antibody functionalized magnetic beads to the immobilized cTnI and also appear to increase the nonspecific interactions between the beads and surface. This is consistent with a model in which the protein becomes irreversibly bound to the membrane surface thus blocking the reaction of the antibodies on the magnetic beads with the surface. Thus, the formation of the protein films on the membrane influenced the performance of the mFDA in several ways, i.e., the sensitivity, background, and total amount of sample that could be filtered was determined by the composition of the filtrate, surface chemistry of the membrane, and pressure of filtration.

Speed and Sensitivity of cTnI Assays

mFDA detects cTnI through a series of antibody-analyte reactions that have been illustrated in Figure 1. The nanoporous membrane was functionalized with a 1:1 mixture of 16A11 and 19C7 monoclonal antibodies that target epitopes at residues 87-92 and 41-49 of cTnI, respectively. A third monoclonal, SDI, was covalently bound to the SPM microbeads and binds to residues 24-40 of cTnI. These monoclonal antibodies were chosen for their low propensity to cross-react with serum and the fact that the regions they bind to cTnI were not susceptible to enzymatic modification. ELISA was carried out using the same set of antibodies and had a sensitivity of approximately 1 ng/ml, which is consistent with previously published results[5]. The sensitivity of the mFDA was 0.1 pg/ml in PBST, which was four orders of magnitude higher than the ELISA. The increased sensitivity and speed of the mFDA presented in Figure 5 appears to be determined by the rate of mass transport of cTnI to the membrane surface and the reaction of the antibody bound to the SPM beads with the cTnI bound to the membrane.

The FDA response in Figure 5 illustrated that a larger fraction of magnetic beads bind to the nanoporous membranes than the sapphire surfaces, despite the fact that the incubation time of the sample with the membranes and sapphire was 300 sec and 4200 sec, respectively. We attribute the increased speed of the membrane assays to the rapid concentration of cTnI on the membrane surface. Transport of the sample through the membranes can be understood in terms of the Peclet number

$$Pe = \frac{V\delta_m}{D},$$

where V is the flow rate through the membrane, $\underline{\mu_m}$ the critical dimension, and D is the diffusion coefficient of the analyte. The Pe of cTnI was found to vary between 100 and 500 for the 100 and 20 nm nanoporous membranes, respectively, indicating that the flux of protein through the membranes was dominated by convection. It is noteworthy that the fraction of beads bound to the membranes was slightly higher for the 100 nm membrane, as shown in Figure 5B, across the range of cTnI concentrations. This result suggests the mFDA sensitivity does not result from selective sieving but rather the flow conditions and reaction at the membrane surface. These results confirm that a significant fraction of cTnI binds to the interface of both the 20 nm and 100 nm membranes that is readily accessible to the SPM beads.

The selection of the membrane pore size had a significant influence on the mFDA performance in samples containing FCS. It was found that the permeability of the 20 nm membranes rapidly decreased in FCS, severely limiting the amount of sample that can filtered and producing very low levels of bead binding. This was attributed to rapid formation of a protein film on the 20 nm pore membranes. This led us to perform the mFDA assays with FCS using 100 nm membranes that were able to reproducibly filter samples containing up to 15% FCS. The total amount of sample filtered through these membranes was self-limiting at approximately 0.15 ml/mm^2.

The specific and nonspecific adhesion of the SPM microbeads to the PEG surfaces in the FDA was found to be highly sensitive to the surface chemistry of the membranes, as shown in Figure 6A. The higher ratios of BOC-PEG:M-PEG produced higher fractions of beads bound to the surface of the membranes. However, increased antibody coverage also led to an increase in the number of beads non-specifically bound to the surfaces, i.e., the background of the mFDA increases from 11 to 39% as the BOC-PEG:M-PEG ratio increases from 1:4 to 1:1, respectively. It appears that the 1:4 BOC:M-PEG ratio produced the best binding to background performance for the mFDA as surfaces formed at a 1:10 BOC:M-PEG ratio resulted in lower bound bead fractions. The improved mFDA sensitivity at high antibody coverage is consistent with polyvalent binding of cTnI to membrane, while the nonspecific binding appears to be associated with nonspecific protein interactions of the antibodies on the PEG monolayer.

The sensitivity of the mFDA was ultimately determined by the affinity of the antibody-analyte reactions used to capture and detect cTnI. Two monoclonal antibodies were used to simultaneously capture cTnI on the membranes to increase the avidity of the capture reaction. Thus, the sensitivity of the mFDA assay was limited by the reaction of the SDI monoclonal antibody on the magnetic beads (Figure 1B, **6**) with cTnI (**5**) bound to the membrane. In a conventional ELISA the on-rate rate (k_{on}) is limited by the rate of diffusion of the cTnI to the antibodies on the surface, and the off-rate (k_{off}) is determined by the antibody-antigen energy of the cTnI-antibody interaction and the rate of diffusion of the reactant. Measurements of k_{on} and k_{off} of antibody-protein interactions with surface plasmon resonance (SPR) indicates these parameters vary between 10^5-10^6 $M^{-1}s^{-1}$ and 10^{-3} -10^{-4} s^{-1}, respectively. The sensitivity of the resulting assay would thus be of the order of magnitude of 10^{-7} to 10^{-9} M (or 10^{-6} to10^{-9} gm/ml of cTnI), which is consistent with our cTnI ELISA results.

The immobilization of the antibody on the magnetic beads in the mFDA changed the reaction kinetics of the antibody-antigen interactions. A unique feature of FDA is that the beads were in continuous contact with the membrane surface due to the 6 femtoNewton force produced by their buoyant weight. Experimental measurements of k_{on}* for single molecule interactions of molecules immobilized on surfaces have been made with atomic force microscope and found to have the form

$$k_{on}^{*} = \frac{1}{\tau C_{eff}},$$

where τ is the characteristic interaction time and C_{eff} is the effective concentration of antibody, which is inversely proportional to the volume of the PEG linker[36]. The k_{on}* for antibodies immobilized on AFM probes thorough 2 kDa PEG linkers was measured to be 10^4-10^6 $M^{-1}s^{-1}$, and was consistent with SPR measurements. The k_{on}* for specific molecular interactions taking place between 200 nm diameter SPM beads have also been measured using light scattering[19]. The on-rate for this aggregation assay was found to be 10^3-10^4 $M^{-1}s^{-1}$ and to be highly dependent on the steric mobility of the receptor and size of the magnetic particles, which strongly influenced the rotational diffusion rate of the beads. The properties of the SPM beads and antibody immobilization chemistries have been optimized in this study to maintain high levels of k_{on}* resulting in rapid binding of the beads to cTnI on the membrane.

Magnetic tweezers have previously been used to study the interactions formed between an antibody functionalized bead and protein A coated surface across a range of concentrations.[20] At high concentrations of cTnI the tight binding of the SPM beads suggested they were immobilized through polyvalent interactions, which is consistent with the antibody-protein A studies. As the concentration of cTnI was decreased to 0.1 pg/ml the maximum density of cTnI that could be immobilized on the membrane decreased to approximately 450 molecules/μm^2, which is the range in which single protein A-antibody interactions that form for a 1 μm SPM bead. Thus, it appears that mFDA detects beads in which multivalent bead-surface interactions are formed.

This can be understood in terms of the rate of bond rupture that takes place due to magnetic force, i.e., Bell's law can be used to determine the dissociation rate of single antibody-antigen bond (*N*) under an applied force (*F*) is

$$\mathrm{N} = exp(-\mathrm{t}\cdot \mathrm{k_{on}} exp(\mathrm{F/f}))$$

where *f* is a scaling force and *t* is time. Single cTnI-antibody bonds can be predicted to rupture in tens of seconds under the picoNewton forces used in this assay, which is too fast to be detected with the force differentiation protocol used in this study, while multiple bonds have a significantly lower dissociation rate.[20] Thus, mFDA's increased sensitivity appears to result from the increased number of antibody-antigen bonds formed between the SPM beads and surface. The sensitivity of the mFDA can be varied by changing steric mobility of the antibodies on the beads or size of the magnetic beads, which influence the number of antibody-antigen interactions, the contact area of the bead with the surface, and rate of rotation of the bead. Higher sensitivities may be achieved if a detection system were used that required a shorter time to characterize the binding state of the SPM beads.

Conclusions

An immunoassay for cTnI has been demonstrated in which the analyte was captured on an antibody functionalized nanoporous membrane and detected with an antibody functionalized SPM bead. The membranes allow the analyte to be rapidly concentrated on a surface, decreasing the reaction time from hours to minutes. The sensitivity of the cTnI assay in 15% fetal calf serum was 0.1 pg/ml and the assay can be completed in <16 minutes. Studies of membrane permeability indicated that the assay performance was highly dependent on protein concentration in the sample and filtration pressure. It was found that high concentrations of serum and high filtration pressures led to fouling of the membrane that blocked the bead-surface reaction. Optimum performance was achieved at 15% serum on a 100 nm membrane when filtration was driven through simple adsorption into a nitrocellulose membrane. The four orders of magnitude increase in sensitivity of this assay resulted from the increased number of antibody interactions on the magnetic bead with the surface bond cTnI analyte. The significantly improved performance of the assay and ease of fluid handling in this assay suggests it may be a good candidate for implementation in a point of care diagnostics in which femtogram/ml sensitivities need to be achieved.[4]

Methods

Materials

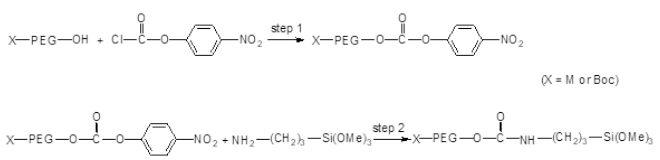

N-methoxyl poly (ethylene glycol)-3-(N-hydroxylsuccinimidyl carboxylate) propionamide (M-PEG-NHS, 2000 g/mol), N-t-butyl carbamate poly (ethylene glycol)-3-(N-hydroxylsuccinimidyl carboxylate) propionamide (Boc-PEG-NHS, 3000 g/mol), α-methoxyl-ω-hydroxyl poly (ethylene glycol) (M-PEG-OH, 2000 g/mol), α -t-butyl carbamate- ω -hydroxyl poly (ethylene glycol) (Boc-PEG-OH, 3000 g/mol) were obtained from Rapp Polymers (Tübingen, Germany). The 4-nitrophenyl chloroformate, dichloromethane (DCM), triethylamine (TEA), diethyl ether (anhydrous), benzene, toluene, 3-aminopropyl trimethoxy silane (3-APTMS), trifluoroacetic acid (TFA), hydrochloric acid (HCl), ammonium hydroxide (NH_4OH), hydrogen peroxide (H_2O_2), sodium phosphate buffer (NaH_2PO_4 and NaHPO4), sodium carbonate buffer (Na_2CO_3 and $NaHCO_3$), ethylenediaminetetraacetic acid (EDTA), polysorbate-20, and fetal calf serum (FCS) were obtained from Sigma-Aldrich Chemicals (St. Louis, MO). Succinimidyl 4-[N-maleimidomethyl]-cyclohexane-1-carboxylate (SMCC) and N-succinimidyl-S-acetylthioacetate (SATA) were sourced from Pierce (Rockford, IL). The polyethylene imine (PEI, Polymin SNA, BASF, Rensseler, NY) was a gift from BASF. The 20 and 100 nm pore size Anodisc® filters were obtained from Whatman (Midstone, Kent, UK), glass pre-filtration filters were obtained from PALL® (Ann Arbor, MI), and the sapphire substrates were obtained from University Wafer (Boston, MA). The human cardiac troponin I (cTnI) was obtained from the National Institute of Standards and Technology (Gathersburg, MD). Two monoclonal anti-cTnI antibodies were obtained from HyTest (Turku, Finland) and will be referred to a 16A11 and 19C7, respectively. A third monoclonal anti-cTnI antibody (SDI) was obtained from Strategic Diagnostic (B9085MA06, Newark, DE). The superparamagnetic microbeads were obtained from MagSense Life Sciences (West Lafayette, IN).

Preparation of polyethylene glycol silane

The PEG-$Si(OCH_3)_3$ compounds were synthesized by a two-step process, as shown in Scheme 1, with either a methoxyl (M) or t-butyl carbamate (Boc) end group. To synthesize M-PEG-silane, the 4-nitrophenyl poly (ethylene glycol) formate (4-NPEG) precursor was first produced by reacting 5.0 g (2.5 mmol) of M-PEG-OH and 2.01 g (10 mmol) of 4-nitrophenyl chloroformate in 30 mL DCM with 2.5 mL (17.5 mmol) of TEA at room temperature for 20 hrs in a nitrogen environment. The resulting hydrochloric acid triethylamine salt (HCl:TEA salt) was separated on filter paper and the product was precipitated three times with cold diethyl ether. The precipitate was dissolved in benzene, filtered, and precipitated again in diethyl ether. The precipitate was dried under vacuum for 3 days at room temperature resulting in a yield of approximately 85%. The M-PEG-$Si(OCH_3)_3$ compound was synthesized by reacting 1.2 g (0.55 mmol) of the 4-NPEG precursor with 0.15 mL (0.83 mmol) of 3-APTMS in 10 mL DCM and 0.39 mL (2.8 mmol) of TEA at room temperature for 72 hrs in a nitrogen environment. The product was purified by crystallization in cold diethyl ether and drying as described above resulting in a yield of approximately 95%.

The Boc-PEG-$Si(OCH_3)_3$ compound was synthesized using a similar approach described for the M-PEG-silane with a final yield of approximately 75 %. All the products were characterized with 1H-NMR and the results are presented in the Supplemental Materials Section.

Scheme 1. Reaction scheme of PEG silane compound

Surface chemistry

The commercial nanoporous alumina membranes and sapphire surfaces were cleaned with concentrated HCl (37.5 %) for 5 min and were then treated with concentrated NH_4OH:H_2O_2 (3 : 1 (v/v)) at 80°C for 30 min. The surfaces were thoroughly rinsed with water, dried in a nitrogen stream, and then dried in a stainless-steel oven at 80°C for at least 2 hrs. The membrane silanization was carried out by reacting 25 mg of Boc-PEG-Si$(OCH_3)_3$ and 100 mg of M-PEG-Si$(OCH_3)_3$ with five membranes in 40ml of dry toluene and 2ml of TEA for 4hrs 17. Excess silane was removed from the membranes by refluxing the surfaces with 40ml toluene for 30 min. The sapphire surfaces were prepared using a similar procedure except lower quantities of silane were used, i.e., 1 mg of Boc-PEG-Si$(OCH_3)_3$ and 4 mg of M-PEG-Si$(OCH_3)_3$ per cm^2 of sapphire of silane per 40 ml of toluene.

The resulting PEG films were covalently functionalized with antibodies via the primary amine groups of the Boc-PEG-Si$(OCH_3)_3$ similar to that described previously[21]. The primary amine was deprotected by reacting the films with TFA for 5 min at room temperature followed by thorough rinsing with water. The amine was then reacted with SMCC in a phosphate buffer (PB: 100mM phosphate buffer) at pH 7.2 for 30min. The SDI and 19C7 anti-cTnI antibodies were modified with sulfhydryl groups using SATA at a 1:10 molar ratio, respectively, in phosphate buffer saline (PBS: PB with 150mM NaCl) and 10mM EDTA at pH 7.2. The sulfhydryl groups were activated with a deacetylation buffer of 50mM hydroxylamine-HCl, 2.5mM EDTA, and 62.5mM Na_2HPO_4-NaH_2PO_4 at pH7.5 for 2 h. This buffer was replaced on an excellulose desalting column with 50mM Na_2HPO_4-NaH_2PO_4 and 1mM EDTA at pH7.2. The active surface of the membrane and sapphire substrate were then reacted with the antibodies. Approximately 3 ml of antibody (conc. 2 mg/ml) was added to an equal volume of PBS solution and reacted with a substrate for 2hr at room temp. Then the surfaces were washed with PBST (PBS with 0.05% Tween-20) and stored until use in the same buffer.

Surface Characterization

Measurements of the chemical properties of the membranes were conducted using an imaging x-photoelectron spectrometer (Axis ULTRA, Kratos, Chestnut Ridge, NY) equipped with a charge neutralization system. Data were collected using a monochromatized Al Kα source (15kV, 300W) at a take-off angle of 60° with respect to the surface. High-resolution spectra were acquired using a pass energy of 40 eV, producing an energy resolution of 0.2 eV. For charge neutralization, the low hybrid mode was used with a 200 mm aperture size and 150 W X-ray power. Typical operating pressures were 10^{-9} torr.

Permeability measurements

The permeability of nanoporous membranes was measured using a technique that has been described previously[28]. Briefly, membranes were placed in a filter holder of defined size and 2ml of solution was filtered through the membrane under a defined pressure. The mass flow rate of PBST, and 10, 15, 20, or 50% FCS in PBST was measured as a function of pressure and time. Each of the FCS solution was pre-filtered with a glass filter to remove any large beads or aggregates in the serum during storage.

Magnetic bead antibody functionalization The superparamagnetic microbeads were functionalized with anti-cTnI monoclonal antibody through a PEG monolayer using the technique similar to that described previously.[20, 21] The beads were first coated with a monolayer of primary amines by physically adsorbing PEI on the negatively charged beads in a sodium carbonate buffer at pH 8.2. The surfaces were then functionalized with a mixed M-PEG-NHS and Boc-PEG-NHS (4:1 wt. ratio) monolayer by reacting the ω-N-hydroxysuccinimidyl ester (NHS) of the PEGs with the primary amine of the PEI coated beads. The PEG modified magnetic beads were subsequently treated with TFA for 5 min to deprotect the primary amine group of the Boc-PEG. The superparamagnetic beads were reacted with 10 mg/ml SMCC in PB, pH 7.2 at a concentration of $2x10^7$ beads per ml. After rinsing in PB the beads were reacted with 2 mg/ml of thiolated 16A11 antibody for 30 min (the anti-cTnI antibody was modified with sulfhydryl groups using SATA as described above).

Force differentiation and bead tracking assays

The FDA was executed using an approach similar to that describe previously.[20, 21] The samples were prepared by spiking 0, 0.1, 1, 5, 10, and 100pg/ml cTnI into 0, 10, 15, and 20% FCS diluted into PBST. These cTnI solutions were prefiltered with the glass filters and then added to either the sapphire or nanoporous alumina membrane surfaces for 5 minutes. Filtration through the membranes took place spontaneously when a piece of filter paper was placed behind the membrane. The magnetic beads were prepared at $3x10^7$ beads/ml concentration in the PBST buffer. These beads were added to the sapphire and membrane surfaces for 5 min. A cover glass placed over the surfaces and a magnetic field of 3000 G and field gradient of 250 G/cm were applied to the membrane surface for 30 sec. The bead distribution on the surfaces was measured using an inverted transmission optical microscope with digital image acquisition (TE300, Nikon, Melville, NY). The microscope made it possible to track the beads and measure their diffusion coefficient.

Conflicts of interest

There are no conflicts to declare.

Acknowledgements

Funding was provided by U.S. Army; Birck Nanotechnology Center at Purdue University; and the Science Foundation of Ireland (08/RP1/B1376 and 08/IN1/B2072). Author Contributions: Performance of experiments and analysis of data: WC, PL, SK, XY, HS, YZ and GL. Wrote the paper: WC, HS, and GL. Designed the study: GL. We would like to acknowledge insightful discussions in the initial stage of preparing this study with Fred Apple, Deborah Sherman and Dmitry Zemlyanov.

References

1. A. S. Jaffe, L. Babuin and F. S. Apple, *J Am Coll Cardiol*, 2006, **48**, 1-11.
2. K. Thygesen, J. S. Alpert and H. D. White, *J Am Coll Cardiol*, 2007, **50**, 2173-2195.
3. M. J. Pugia and C. P. Price, in *Point-of-care Testing*, eds. C.

P. Price, A. St. John and J. M. Hicks, AACC Press, Washington, DC, 2 edn., 2004, ch. 13-30.
4. W. U. Dittmer, T. H. Evers, W. M. Hardeman, W. Huijnen, R. Kamps, P. de Kievit, J. H. Neijzen, J. H. Nieuwenhuis, M. J. Sijbers, D. W. Dekkers, M. H. Hefti and M. F. Martens, *Clinica chimica acta; international journal of clinical chemistry*, 2010, **411**, 868-873.
5. F. S. Apple, L. A. Pearce, S. W. Smith, J. M. Kaczmarek and M. M. Murakami, *Clin Chem*, 2009, **55**, 930-937.
6. X. Fu, Y. Wang, Y. Liu, H. Liu, L. Fu, J. Wen, J. Li, P. Wei and L. Chen, *The Analyst*, 2019, **144**, 1582-1589.
7. Z. Cheng, R. Wang, Y. Xing, L. Zhao, J. Choo and F. Yu, *The Analyst*, 2019, **144**, 6533-6540.
8. O. Poetz, T. Dieze, H. Hammer, F. Weiss, C. Sommersdorf, M. F. Templin, C. Esdar, A. Zimmermann, S. Stevanovic, J. Bedke, A. Stenzl and T. O. Joos, *Analytical chemistry*, 2018, **90**, 5788-5794.
9. P. O'Brien, *Toxicology*, 2008, **245**, 206-218.
10. T. Braun, M. K. Ghatkesar, N. Backmann, W. Grange, P. Boulanger, L. Letellier, H. P. Lang, A. Bietsch, C. Gerber and M. Hegner, *Nat Nanotechnol*, 2009, **4**, 179-185.
11. S. J. Osterfeld, H. Yu, R. S. Gaster, S. Caramuta, L. Xu, S. J. Han, D. A. Hall, R. J. Wilson, S. Sun, R. L. White, R. W. Davis, N. Pourmand and S. X. Wang, *Proc Natl Acad Sci U S A*, 2008, **105**, 20637-20640.
12. R. McKendry, J. Zhang, Y. Arntz, T. Strunz, M. Hegner, H. P. Lang, M. K. Baller, U. Certa, E. Meyer, H. J. Guntherodt and C. Gerber, *Proc Natl Acad Sci U S A*, 2002, **99**, 9783-9788.
13. D. R. Baselt, G. U. Lee, M. Natesan, S. W. Metzger, P. E. Sheehan and R. J. Colton, *Biosens Bioelectron*, 1998, **13**, 731-739.
14. J. R. Lee, I. Appelmann, C. Miething, T. O. Shultz, D. Ruderman, D. Kim, P. Mallick, S. W. Lowe and S. X. Wang, *Theranostics*, 2018, **8**, 1389-1398.
15. B. Lim, S. R. Torati, K. W. Kim, X. Hu, V. Reddy and C. Kim, *Npg Asia Mater*, 2017, **9**.
16. B. Lim, V. Reddy, X. Hu, K. Kim, M. Jadhav, R. Abedini-Nassab, Y. W. Noh, Y. T. Lim, B. B. Yellen and C. Kim, *Nat Commun*, 2014, **5**.
17. A. Ranzoni, G. Sabatte, L. J. van Ijzendoorn and M. W. Prins, *ACS nano*, 2012, **6**, 3134-3141.
18. C. S. Thaxton, R. Elghanian, A. D. Thomas, S. I. Stoeva, J. S. Lee, N. D. Smith, A. J. Schaeffer, H. Klocker, W. Horninger, G. Bartsch and C. A. Mirkin, *Proc Natl Acad Sci U S A*, 2009, **106**, 18437-18442.
19. J. Baudry, C. Rouzeau, C. Goubault, C. Robic, L. Cohen-Tannoudji, A. Koenig, E. Bertrand and J. Bibette, *Proc Natl Acad Sci U S A*, 2006, **103**, 16076-16078.
20. H. Shang and G. U. Lee, *Journal of the American Chemical Society*, 2007, **129**, 6640-6646.
21. G. U. Lee, S. Metzger, M. Natesan, C. Yanavich and Y. F. Dufrene, *Anal Biochem*, 2000, **287**, 261-271.
22. P. Li, D. Gandhi, M. Mutas, Y. F. Ran, M. Carr, S. Rampini, W. Hall and G. U. Lee, *Nanoscale*, 2020, DOI: 10.1039/c9nr10362g.
23. Y.-F. Ran, C. Fields, J. Muzard, V. Liauchuk, M. Carr, W. Hall and G. U. Lee, *Analyst*, 2014, **139**, 6126-6134.
24. G. F. Blackburn, H. P. Shah, J. H. Kenten, J. Leland, R. A. Kamin, J. Link, J. Peterman, M. J. Powell, A. Shah, D. B. Talley and et al., *Clin Chem*, 1991, **37**, 1534-1539.
25. S. Kamara, Q. H. Tran, V. Davesne, G. Felix, L. Salmon, K. Kim, C. Kim, A. Bousseksou and F. Terki, *Adv Mater*, 2017, **29**.
26. S. P. Mulvaney, K. M. Myers, P. E. Sheehan and L. J. Whitman, *Biosens Bioelectron*, 2009, **24**, 1109-1115.
27. R. L. Edelstein, C. R. Tamanaha, P. E. Sheehan, M. M. Miller, D. R. Baselt, L. J. Whitman and R. J. Colton, *Biosens Bioelectron*, 2000, **14**, 805-813.
28. S. W. Lee, H. Shang, R. T. Haasch, V. Petrova and G. U. Lee, *Nanotechnology*, 2005, **16**, 1335-1340.
29. R. C. Furneaux, W. R. Rigby and A. P. Davidson, *Nature*, 1989, **337**, 147-149.
30. Z. Wang, R. T. Haasch and G. U. Lee, *Langmuir*, 2005, **21**, 1153-1157.
31. L. J. Zeman and A. L. Zydney, *Microfiltration and ultrafiltration : principles and applications*, M. Dekker, New York, 1996.
32. W. M. Deen, *Aiche Journal*, 1987, **33**, 1409-1425.
33. W. S. Opong and A. L. Zydney, *Aiche Journal*, 1991, **37**, 1497-1510.
34. H. Brenner and L. J. Gaydos, *Journal of Colloid and Interface Science*, 1977, **58**, 312-356.
35. C. Rankl, F. Kienberger, L. Wildling, J. Wruss, H. J. Gruber, D. Blaas and P. Hinterdorfer, *Proc Natl Acad Sci U S A*, 2008, **105**, 17778-17783.
36. L. Cohen-Tannoudji, E. Bertrand, J. Baudry, C. Robic, C. Goubault, M. Pellissier, A. Johner, F. Thalmann, N. K. Lee, C. M. Marques and J. Bibette, *Phys Rev Lett*, 2008, **100**, 108301.

ARTICLE

TOC Figure. Schematic of the loading of superparamagnetic beads (red spheres) into a nanoporous membrane (orange membrane) in a lab on a chip device with window (on top) for the rapid and ultrasensitive detection of cardiac troponin I.